Application of a "slice" proper orthogonal decomposition to the far field of an axisymmetric turbulent jet

Stephan Gamard and William K. George
Turbulence Research Laboratory, Department of Thermo and Fluid Dynamics, Chalmers University of Technology, SE-41 296 Gothenburg, Sweden

Daehan Jung
Department of Mechanical Engineering, Korean Air Force Academy, Cheongwon, Chungbuk 363-849, Korea

Scott Woodward
Department of Mechanical and Aerospace Engineering, University at Buffalo, Buffalo, New York 14260

(Received 24 September 2001; accepted 4 March 2002; published 5 June 2002)

Instantaneous measurements of the streamwise velocity component were obtained in the far field region of an axisymmetric turbulent jet at exit Reynolds numbers ranging from 40 000 to 84 700. The data were taken from 20 to 69 diameters downstream of the jet exit using 138 hot-wires. The proper orthogonal decomposition was applied to a double Fourier transform in time and azimuthal direction of the two-point velocity correlation tensor. The first eigenspectrum, which contains more than 60% of the kinetic energy, has two peaks: A dominant peak at azimuthal mode-2 at near zero frequency, and a secondary peak at mode-1 at a local Strouhal number (fx/U_c) of approximately 1. The most striking feature was the general behavior of the eigenspectra: when normalized to reflect the energy repartition per mode number only, they peaked at mode-2, and were independent of downstream position in the experiment considered. They were also similar in nature to those obtained in earlier experiments at $x/D=6$, just past the end of the potential core, but distinctly different from those closer to the jet exit where mode-0 and higher modes dominated. © *2002 American Institute of Physics.* [DOI: 10.1063/1.1471875]

I. INTRODUCTION

Earlier experiments on turbulent jets (Crow and Champagne,[1] Brown and Roshko[2]) made clear that large structures dominated the physics of the axisymmetric jet. Although no clear mathematical definition of those structures is widely accepted, their presence is not contested (see Cantwell[3] or Hussain[4] for a review).

Most studies on the large-scale structures in the axisymmetric turbulent jet concentrated on the potential core region, in part because of its interest for noise-production, but also because of the limitations of flow visualization. In the 1980's, the proper orthogonal decomposition (POD, Lumley[5]) was applied to this flow field. Because of the large amount of data required and technical limitations, these efforts were confined to a single downstream position ($x/D=3$) in the near jet mixing layer (see Glauser,[6] Glauser and George[7]). More recently, Citriniti and George[8] designed a 138-probe array, specifically to resolve the instantaneous velocities in a cross section at a distance of three diameters downstream. The array used very long wires to minimize the spatial aliasing which results from turbulence scales smaller than the separation of the hot-wires. They showed that the first eigenvalue of this ''slice'' POD was able to account for 66% of the kinetic energy field, and that azimuthal mode numbers 0 and 6 dominated the dynamics of the flow, consistent with the earlier results of Glauser and George.[7]

Jung[9] (see also Jung *et al.*[10]) used the same 138-wire probe to investigate the near field region of the jet, from $2 \leqslant x/D \leqslant 6$. He was able to show that the earlier experiments were carried out at sufficiently high Reynolds number to ensure the independence of the resolved scales from it. Also, he discovered that the eigenspectra evolved in the jet mixing layer with downstream distance. Specifically, there was a decrease of the axisymmetric mode, and a progressive shift of the secondary peak from mode-6 at 2 to 3 diameters downstream, to mode-2 by the end of the potential core region. The energy fraction per mode number above mode-0 collapsed when nondimensionalized with shear layer variables: distance downstream, and exit velocity. A similar POD evolution with downstream distance has also been observed in higher Mach numbers in the recent experiments of Ukeiley *et al.*[11] using a smaller probe array.

Much more is known analytically about the far field region of the jet due to the simplifications offered by a properly done similarity analysis (see the appendix in Hussein *et al.*[12]) The single point LDA and flying hot-wire measurements of Hussein *et al.*[12] and Panchapakesan and Lumley[13] among others, have contributed substantially to understanding the single point statistics. There is a considerable lack of knowledge, however, about the evolution of the large scale structures in the far field region. What is known is derived mostly from flow visualization and conditional sampling studies. Mungal and Hollingsworth[14] using the exhaust plume of a TITAN IV rocket fired in the upward direction observed organized structures at very high Reynolds number,

2×10^8, similar to those observed in laboratory experiments at Reynolds numbers of 10^4. Dimotakis *et al.*,[15] using laser-induced fluorescence, investigated the far field of an axisymmetric jet up to 160 diameters at low Reynolds numbers (mostly 500–600), and concluded that the coherent structures' azimuthal distribution must be dominated by axisymmetric (mode-0) or helical (mode-1) modes. Yoda *et al.*[16,17] used planar flow visualizations and measured concentration fields in a round jet at Reynolds numbers of 1000–5000. They observed both axisymmetric and helical modes in the far field of the jet, and concluded that the structures actually evolve in a pair of counter-rotating spirals, or ±1 modes. Tso and Hussain[18] using an array of hot-wires studied the behavior of large-scale structures in the far field of a round jet at high Reynolds number, but their measurement apparatus could only account for axisymmetric (mode-0), helical ($m=\pm1$), and double-helical ($m=\pm2$) structures.

The bias of previous experiments in looking only for structures with a very low azimuthal mode number is directly linked to the earlier analytical studies. In particular, Batchelor and Gill[19] and Michalke[20–22] used a linear stability analysis of a parallel axisymmetric free shear flow to conclude that mode-1 (helical mode) should dominate the flow field in the far jet region. For the near jet where a potential core still exists with a flat region in the velocity profile, mode-0 and 1 could grow together with mode-0 dominating. Unfortunately, experiments designed to find only mode-0 or mode-1 usually find only those modes, because of the spatial aliasing of the higher (unresolved) modes into the lower ones. This problem was discussed in detail in Glauser and George[23] and avoided here.

The experiment described herein uses the experimental apparatus of Citriniti and George[8] and Jung[9] to study the far field region of the jet from $20\leqslant x/D\leqslant69$. The 138-wire array resolves the azimuthal distribution up to 16 mode numbers, and removes by spatial and temporal filtering the higher modes so the energy from them is not aliased into the lower ones. Of particular interest is how the POD eigenspectra change with downstream distance, and their relation (if any) with the near jet results.

II. EXPERIMENT AND APPARATUS

The experimental facilities: the turbulent jet apparatus, the 138 hot wires probe array with corresponding anemometers, and data acquisition system have all been extensively used and are thoroughly described in Citriniti and George[8] and Jung.[9] Only the key features will be repeated here.

The hot-wires array (Fig. 1) was comprised of six concentric radii of hot wires, with an increasing number of hot-wires per radius (Fig. 2). Each single long hot-wire, 1 cm long and made of unplated 12.7 μm tungsten wire, was oriented to measure the downstream component of the velocity. The length of the wire was chosen to remove the small physical scales by spatially low-pass filtering, so as not to alias them (Glauser and George[23]). Those scales removed are of no interest in our study of the large scale behavior of the flow (see Citriniti and George[24] for details). The data were sampled at 4 kHz for all configurations, which is higher than the temporal Nyquist criterion, and measurements were made simultaneously at all 138 positions. Each block had 4096 samples, and a total of 400 blocks of data were taken per configuration, yielding a variability of less than 5% for the cross-spectra used in the POD.

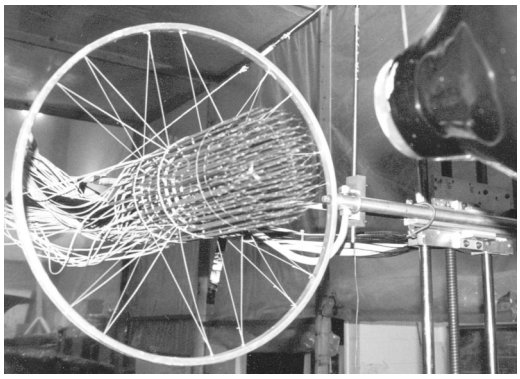

FIG. 1. The jet facility.

Since the probe array size was fixed, jets of two different diameters (2.54 and 1 cm, respectively) were used to be able to measure at different relative positions downstream. The 1/2 radius of the probe was matched with $r_{1/2}$ (the radial position where the flow velocity has reached half the centerline amplitude). Extra positions were added, closer to the optimized ones or farther away, to check the effect on the eigenvalues of not covering the totality of the cross-section. Table I summarizes the experimental configurations.

III. POD DECOMPOSITION

Despite having been introduced to the fluid mechanics community more than 30 years ago by Lumley,[5] the technique known as the proper orthogonal decomposition (POD in short) has been used extensively only very recently in free shear flow experiments, starting with the work of Glauser,[6] mainly due to the computer power required to apply it. Simply put, when applied to experimental data, the POD can be viewed as a filtering device used to objectively eliminate the low energy motions of the flow that are obscuring the main energetic features of the flow (George[25]).

Mathematically, the proper orthogonal decomposition projects the random velocity $u_i(\underline{x},t)$ into an orthonormal coordinate system $\phi_i(\underline{x},t)$ (Holmes *et al.*[26]). The projection is optimal in the sense that the first projection captures most of the energy; or mathematically speaking, the projection of the velocity field into the function $\phi_i(\underline{x},t)$ has to have the maximal amplitude. Accordingly, we are interested in the scalar:

$$\alpha=\frac{\int u_i(\underline{x},t)\phi_i^*(\underline{x},t)d\underline{x}dt}{\left[\int\phi_i(\underline{x},t)\phi_i^*(\underline{x},t)d\underline{x}dt\right]^{1/2}}, \tag{1}$$

where the asterisk represents a complex conjugate.

Since the optimization should first be independent of the sign of the velocity and valid in a statistical sense we should, therefore, maximize $\overline{\alpha^2}=\lambda$ and not α only. This is achieved by solving the integral equation (see Jung[9] for details)

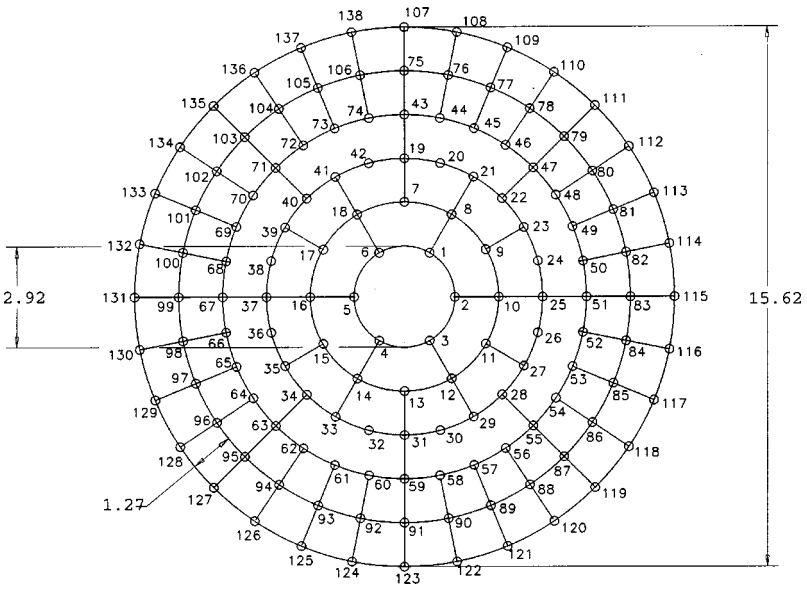

FIG. 2. The 138 hot-wire probe array. Each dot represents a single hot-wire.

$$\int R_{ij}(\underline{x},\underline{x}',t,t')\phi_j(\underline{x}',t')d\underline{x}'dt' = \lambda\phi_i(\underline{x},t), \tag{2}$$

where R_{ij} is the two-point velocity correlation tensor

$$R_{ij}(\underline{x},\underline{x}',t,t') = \overline{u_i(\underline{x},t)u_j^*(\underline{x}',t')}. \tag{3}$$

If the integration is over a finite field, then the solution to Eq. (2) can be found by the means of the Hilbert–Schmidt theory, since the kernel of the equation, R_{ij}, is Hermitian symmetric. When dealing with a periodic or stationary dimension, both of which are the case for the axisymmetric jet considered here, it is better (Lumley,[5] George[25,27]) to first Fourier transform the velocity field in those particular directions, then apply the POD to the transformed field. The results produce then, at each downstream location, x, for each POD mode, n, an eigenspectrum, $\lambda^{(n)}(m,f)$, and eigenfunctions, $\phi_i^{(n)}(r,m,f)$, each functions of mode number, m, and frequency, f, and the latter also a function of the radius, r.

The application of the POD to the doubly Fourier transformed field has the following properties (restricted here for the sake of compactness to the longitudinal velocity component only, at a given fixed downstream position):

(i) There exists not one, but a denumerable set of solutions to Eq. (2):

$$\int R_{11}(x,r,r',m,f)\phi_1^{(n)*}(x,r',m,f)r'dr' = \lambda^{(n)}(x,m,f)\phi_1^{(n)}(x,r,m,f), \quad (n=1,2,3\ldots). \tag{4}$$

Note that the r in the integral is the Jacobian for the cylindrical coordinate system.

(ii) The eigenfunctions are orthonormal (and therefore form a basis for this space)

$$\int \phi_1^{(p)}(x,r,m,f)\phi_1^{(q)}(x,r,m,f)rdr = \delta_{p,q}, \tag{5}$$

with $\delta_{p,q}$ being the Kronecker delta function.

(iii) The velocity field can be expanded in this system

$$u_1(x,r,m,f) = \sum_n a_n(x,m,f)\phi_1^{(n)}(x,r,m,f), \tag{6}$$

with

$$a_n(x,m,f) = \int u_1(x,r,m,f)\phi_1^{(n)*}(x,r,m,f)rdr. \tag{7}$$

(iv) The above coefficients are uncorrelated

$$\overline{a_n a_m^*} = \lambda^{(n)}\delta_{n,m}. \tag{8}$$

(v) The double correlation velocity tensor can be expressed into a convergent double series

TABLE I. Jet parameters.

	2.54 cm diam						1 cm diam					
x/D	20		21		22		46		54		69	
Velocity (m/s)	40	50	40	50	40	50	60	70	60	70	60	70
Reynolds #	67 700	84 700	67 700	84 700	67 700	84 700	40 000	46 700	40 000	46 700	40 000	46 700
$(U/U_c)_{\min}$ (%)	8.81		11.64		14.65		10.29		19.88		35.56	

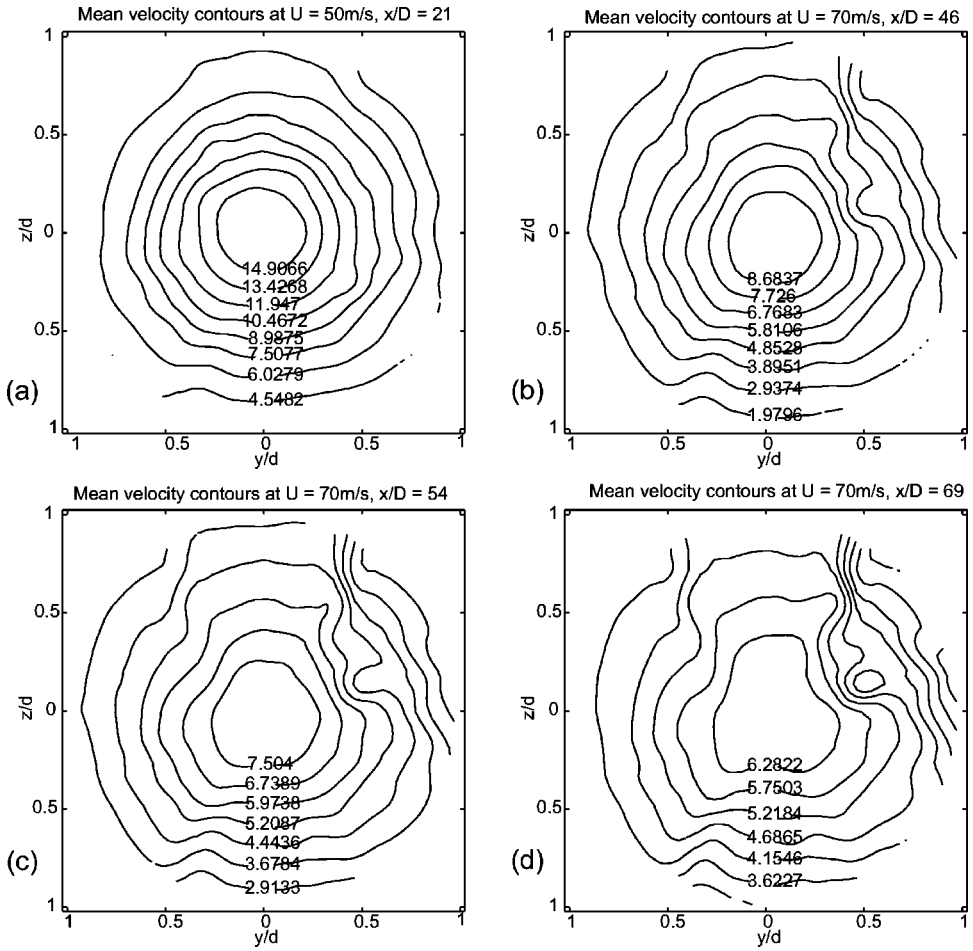

FIG. 3. Mean velocities at different downstream positions: (a) $x/D=21$ ($Uo=50$ m/s), and (b) 46, (c) 54, (d) 69 (last 3 at $Uo=70$ m/s).

$$R_{11}(x,r,r',m,f)=\sum_n \lambda^{(n)}(x,m,f)\,\phi_1^{(n)}(x,r,m,f)\times\phi_1^{(n)*}(x,r',m,f). \tag{9}$$

(vi) The eigenvalues are ordered and their sum is equal to the kinetic energy

$$\lambda^{(1)}>\lambda^{(2)}>\lambda^{(3)}\cdots>0, \tag{10}$$

$$E=\int_f\int_r\sum_m \overline{u_1(x,r,m,f)u_1^*(x,r,m,f)}\,r\,dr\,df$$

$$=\sum_n\sum_m\int_f\lambda^{(n)}(x,m,f)\,df. \tag{11}$$

The power of the POD can be seen in the last two equations, since the eigenfunctions order the flow in an energetic sense and allow the most energetic features of the flow to be seen directly. As noted by Glauser and George[23] and Citriniti and George,[8] only a few eigenvalues are necessary to capture most of the energy for the jet, so the method is experimentally viable.

IV. STATISTICAL RESULTS

Before applying the POD, we checked the validity of our results by studying the mean statistical properties of the measurements. Contour maps of the velocity were computed and a sample is reproduced in Fig. 3. The profile closest to the exit, at $x/D=21$ is clearly axisymmetric, but as the probe is moved farther downstream, it appears to develop a "dimple" at $\theta\simeq 80°$, because one probe is obviously slightly miscalibrated in the 1 cm jet. The mean flow results are highly sensitive to proper calibration and drift in the anemometers, especially in such a high turbulence intensity flow field. (It is not a trivial task to maintain 138-wires operating simultaneously.) If this single probe is removed from consideration, the profiles are axisymmetric to within few percents. As is well-known (see Hussein *et al.*[12]), hot-wires do not give highly accurate results for turbulence intensities above 25%. In the far field region of the jet, the minimum intensity is 28% at the centerline and reaches 100% at the outer radial position. It is not expected, however, that the modal content of the turbulence, which is of primary interest here, will be significantly affected by these errors.

V. POD RESULTS

The eigenspectra show how the energy is distributed with azimuthal mode number, m, and frequency, f, at a given downstream position, x. Therefore they demonstrate how the main characteristics of the flow evolve. The first eigenspectrum contains more than 60% of the flow energy, consistent with results of Citriniti and George[8] and Jung *et al.*[10] for the jet near the source. Note that actually the term energy here only refers to the downstream component of the

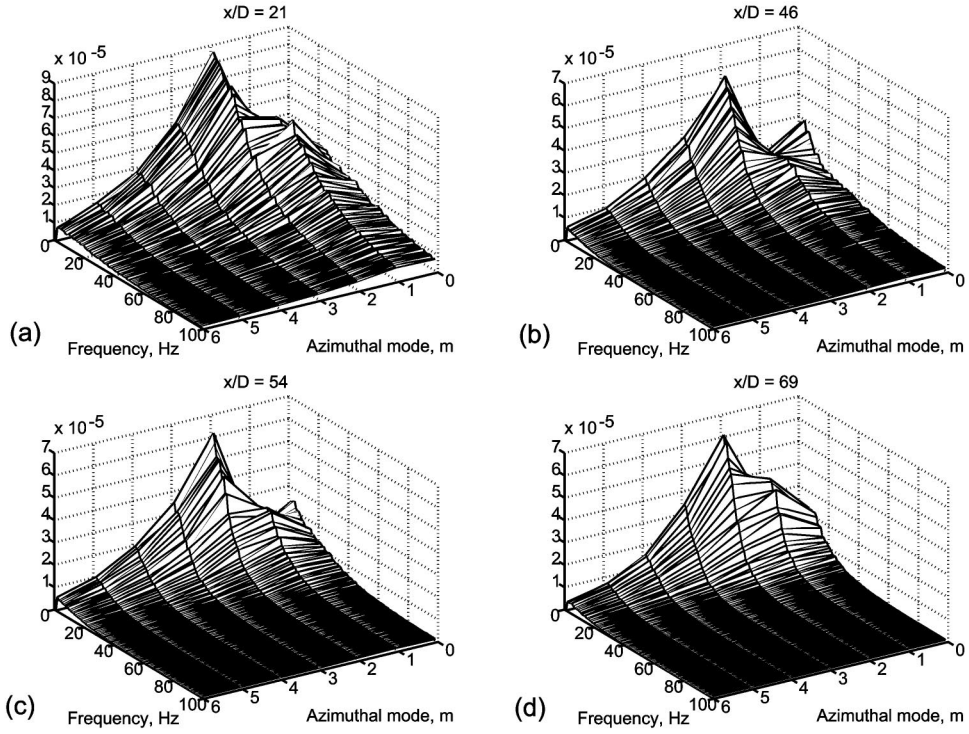

FIG. 4. Eigenspectrum function of azimuthal mode number (m) and frequency (f) at different positions: (a) $x/D=21$ ($Uo=50$ m/s), and (b) 46, (c) 54, (d) 69 (last 3 at $Uo=70$ m/s).

kinetic energy, since the apparatus is designed to measure the streamwise component of the instantaneous velocity only.

Contour plots of the eigenspectrum for the first POD mode are presented in Fig. 4 for several downstream positions for fixed upstream conditions. The energy is concentrated at very low frequencies and in a few mode numbers. Interestingly, the shape of the eigenspectra does not evolve with downstream distance. All show a peak in amplitude at very low frequency for azimuthal mode-2, and a secondary peak at a slightly higher frequency for azimuthal mode-1. The plots in Fig. 5 show these features more clearly, since contour figures are presented alongside with three-dimensional (3D) plots. The latter plots are shown using the local Strouhal numbers instead of frequency, i.e., $\mathrm{St}=fx/U_c$, where U_c is the centerline velocity. The four pictures are strikingly similar, all showing a peak for azimuthal

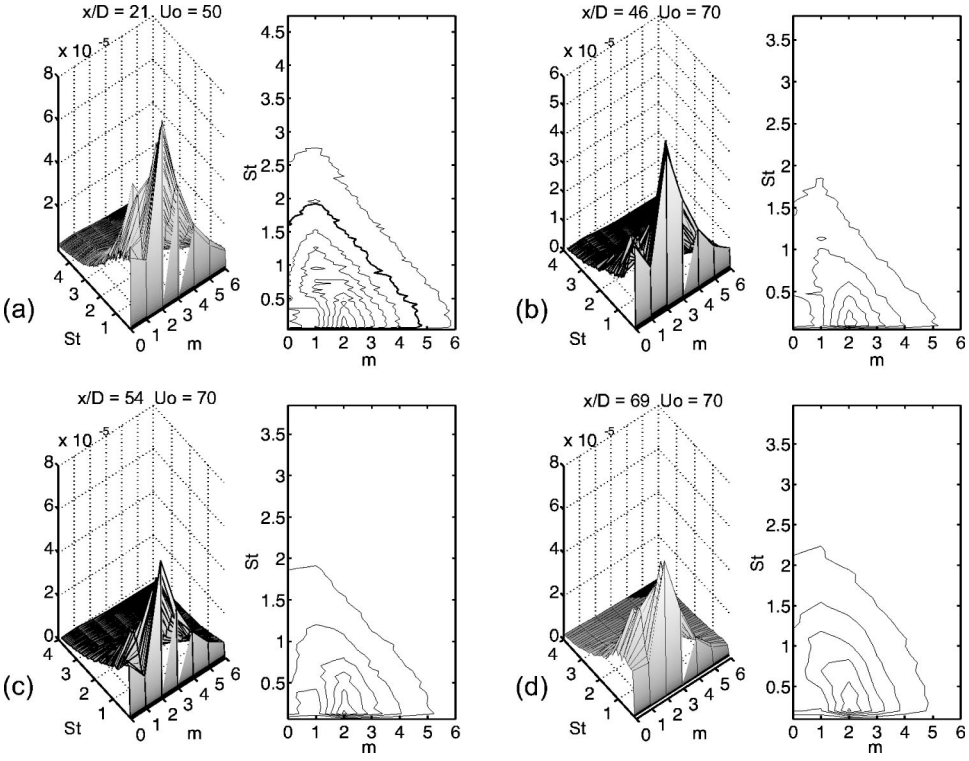

FIG. 5. Eigenspectrum function of azimuthal mode number (m) and Strouhal number ($St=f\cdot x/Uc$) at different positions: (a) $x/D=21$ ($Uo=50$ m/s), and (b) 46, (c) 54, (d) 69 (last 3 at $Uo=70$ m/s).

TABLE II. Relative energy (%) in the azimuthal direction only for the first POD mode.

	6D	20D		21D		22D		46D		54D		69D	
m	24 m/s	40 m/s	50 m/s	40 m/s	50 m/s	40 m/s	50 m/s	60 m/s	70 m/s	60 m/s	70 m/s	60 m/s	70 m/s
0	7.78	11.09	10.40	11.23	10.54	11.38	10.85	10.87	11.26	10.08	10.71	10.01	10.64
1	11.09	14.29	14.19	14.23	14.05	14.11	14.20	12.24	13.01	11.84	12.41	13.63	13.75
2	12.15	14.93	14.70	14.82	14.45	14.50	14.77	14.29	14.58	14.98	14.79	15.22	15.07
3	11.04	8.23	8.50	8.30	8.46	8.26	8.48	7.97	7.81	8.76	8.43	8.97	8.70
4	7.74	5.01	5.18	4.97	5.20	5.03	5.10	5.01	4.87	5.30	5.26	5.28	5.19
5	4.82	3.18	3.28	3.13	3.29	3.17	3.16	3.30	3.17	3.43	3.29	3.26	3.16
6	2.98	1.88	1.94	1.90	1.94	1.92	1.90	2.01	1.90	2.15	2.05	2.05	1.99
7	1.92	1.30	1.32	1.29	1.31	1.30	1.30	1.38	1.31	1.45	1.41	1.40	1.35
8	1.32	0.92	0.94	0.92	0.94	0.93	0.92	1.00	0.95	1.06	1.01	1.03	0.98
9	0.96	0.69	0.71	0.68	0.71	0.70	0.69	0.77	0.74	0.81	0.77	0.79	0.75
10	0.73	0.55	0.56	0.55	0.56	0.55	0.54	0.62	0.60	0.65	0.62	0.65	0.61
11	0.58	0.46	0.46	0.45	0.46	0.45	0.45	0.53	0.52	0.55	0.53	0.55	0.52
12	0.47	0.32	0.31	0.32	0.33	0.33	0.32	0.39	0.35	0.45	0.41	0.47	0.43
13	0.41	0.28	0.27	0.28	0.28	0.29	0.28	0.36	0.32	0.41	0.37	0.43	0.39
14	0.38	0.25	0.25	0.26	0.27	0.27	0.26	0.33	0.30	0.38	0.35	0.40	0.36
15	0.36	0.25	0.25	0.26	0.27	0.26	0.25	0.33	0.29	0.37	0.33	0.39	0.36
SUM	64.73	63.63	63.24	63.60	63.06	63.46	63.47	61.41	61.98	62.67	62.72	64.54	64.25

mode-2 at near zero Strouhal number, and a secondary peak for azimuthal mode-1 and a Strouhal number of around 1. This near similarity is a reassuring check on the accuracy of the measurements, since the eigenspectra must obey equilibrium similarity equations (Ewing[28]), and can be shown to collapse when properly normalized (Gamard and George[29]).

It should be noted that the high turbulence intensity of this flow precludes the simple application of Taylor's frozen field hypothesis to the experimental results. Because of the unsteady convection velocity and the strong mean shear, ''frequency'' cannot be simply interpreted as temporal or spatial, but is a contribution of both (Lumley[30]). Or, in other words, it is not obvious what the proper convection velocity is without detailed considerations (cf. Wills,[31] Zaman, and Hussain[32]).

A key property of the eigenspectra is its ability to show how the kinetic energy of the flow is distributed among the various azimuthal modes [following Eq. (11)]. The energy distribution per azimuthal mode number, m, is given by the quantity

$$\xi^{(n)}(x,m)=\frac{\int_f \lambda^{(n)}(x,m,f)\,df}{\Sigma_m \int_f \lambda^{(n)}(x,m,f)\,df}, \tag{12}$$

where the denominator is actually the total kinetic energy for the downstream component of the velocity according to Eq. (11). Data are shown in Table II, and results are plotted in Fig. 6 for the first eigenspectra ($n=1$). It was expected that the far field results would not change with downstream distance, since they are described by equilibrium similarity. The minor differences between the profiles are due to the difference in coverage of the cross-section of the flow of the fixed probe array, as explained in Gamard and George.[29]

Figure 7 compares the present results with the near-field result made at the end of the potential core region ($x/D=6$) by Jung.[9] Although the evolution from the mode-0 dominance at $x/D=3$ to the mode-2 dominance of the far jet is not quite complete by $x/D=6$, both show the same key

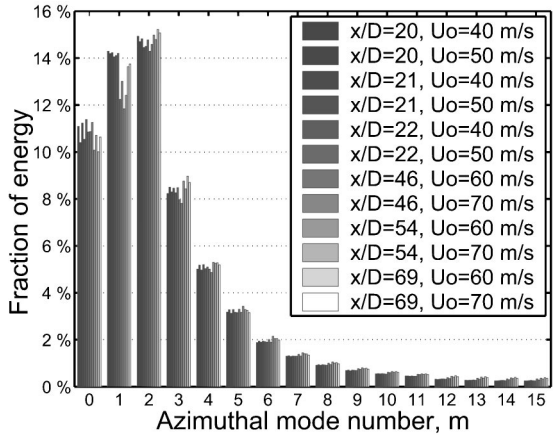

FIG. 6. Relative fraction of energy contained in the first eigenspectrum as a function of mode number, far jet cases.

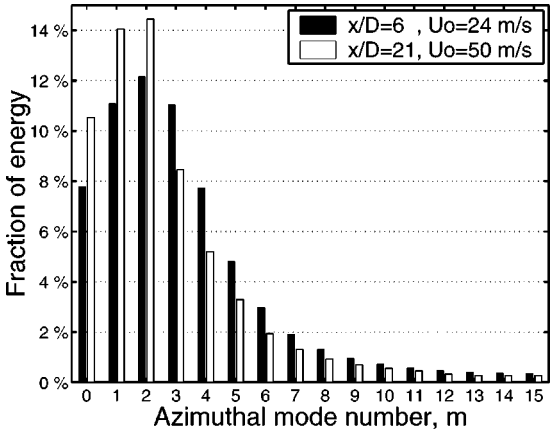

FIG. 7. Relative fraction of energy contained in the first eigenspectrum as a function of mode number, comparison between results at the end of the potential core and far jet results.

feature, namely the dominance of azimuthal mode-2.

Azimuthal mode-1 accounts for 13% on average, and mode-2 for slightly less than 15%. These results are contrary to commonly accepted results of a dominance of helical (mode-1) structures. The reason is most likely that earlier experimental apparatus lacked the resolution to measure more than very few azimuthal modes. Since there was no spatial filtering, the unresolved modes were aliased into the lower ones, thereby distorting the low mode number energy distribution. Further complicating the flow visualization studies is the fact that it is very difficult to distinguish between mode-1 and mode-2 simply visually. Finally, many of the earlier studies were made at Reynolds numbers well below those reported here.

VI. SUMMARY AND CONCLUSION

Measurements in the far field of an axisymmetric turbulent jet were taken with a 138 hot-wire probe array. The experiment covered downstream distances from 20 to 69 diameters, and Reynolds numbers from 40 000 to 84 700. The proper orthogonal decomposition was applied to "slices" (or cross-sections) of the flow. The resulting eigenspectra are a measure of how the energy is partitioned in the flow. They show clearly two distinct peaks: One at near zero frequency at azimuthal mode-2, and the other at azimuthal mode-1 for a local Strouhal number (fx/U_c) of approximately 1. When integrated to remove the frequency dependence, and normalized by the kinetic energy of the downstream velocity component, it was shown that the first eigenspectrum accounts for more than 60% of the energy. The normalized eigenspectra do not depend on downstream distance in the equilibrium similarity region, and are very close to results obtained earlier at the end of the potential core region.

The results presented here can be compared to analytical stability results of Batchelor and Gill,[19] Michalke.[21,22] As noted by Jung *et al.*,[10] the evolution of the near jet is qualitatively in agreement with these stability results, a surprising finding in view of the very high Reynolds number of this fully turbulent flow. It is possible that a nonlinear and/or nonparallel stability analysis might predict the eventual dominance of mode-2. This could explain the similarity between the profiles taken at different downstream positions, and those recently taken in the wake of an axisymmetric disk by Johansson *et al.*,[33] or might eventually lead to an explanation of sound measurements by Kopiev *et al.*,[34] who found azimuthal mode-2 sound sources past the end of the potential core.

The results obtained here can be contrasted with previous experimental results, which showed a predominance of azimuthal mode-1 instead of the predominance of azimuthal mode-2 found here. This is likely because experimental apparatus limited the resolution to a maximum of mode-2, thereby aliasing the higher modes into the lower ones. This problem was discussed in detail in Glauser and George,[23] and was avoided in the present experiment by the large probe array.

Interestingly, Morris *et al.*[35] developed a model for turbulent shear-flows based on instability waves, and predicted a peak of the spectrum in the far-field at a local Strouhal number of 1, just as we are observing. Our results also bear an interesting resemblance to the theoretical results of Chan.[36] Thus there are strong hints that modeling using stability ideas for a non-parallel shear layer might succeed in reproducing all the key features observed here.

ACKNOWLEDGMENTS

This work was initiated at the Turbulence Research Laboratory of the State University of New York at Buffalo, and continued with the move of TRL to Chalmers University of Technology in Gothenburg, Sweden. This work was initially supported by the U.S. Air Force Office of Scientific Research under Grant No. F49620-98-1-0143, and by the USA National Science Foundation under Grant No. CTS-974367. It continues with the support of the Swedish Research Council Grant No. 2641.

[1] S. C. Crow and F. H. Champagne, "Orderly structure in jet turbulence," J. Fluid Mech. **48**, 547 (1971).
[2] G. L. Brown and A. Roshko, "On density effects and large structure in turbulent mixing layers." J. Fluid Mech. **64**, 775 (1974).
[3] B. J. Cantwell, "Organized motion in turbulent flows," Annu. Rev. Fluid Mech. **13**, 457 (1981).
[4] A. K. M. F. Hussain, "Coherent structures—reality and myth," Phys. Fluids **26**, 2816 (1983).
[5] J. L. Lumley, "The structure of inhomogeneous turbulent flows," in *Atmospheric Turbulence and Radio Wave Propagation*, edited by A. M. Yaglom and V. I. Tatarsky (Nauka, Moscow, USSR, 1967).
[6] M. N. Glauser, Ph.D. thesis, Department of Mechanical and Aerospace Engineering, State University of New York at Buffalo, 1987.
[7] M. N. Glauser and W. K. George, "Orthogonal decomposition of the axisymmetric jet mixing layer including azimuthal dependence," in *Advances in Turbulence*, edited by G. Comte-Bellot and J. Mathieu (Springer-Verlag, Berlin, 1987), pp. 357–366.
[8] J. H. Citriniti and W. K. George, "Reconstruction of the global velocity field in the axisymmetric mixing layer utilizing the proper orthogonal decomposition," J. Fluid Mech. **418**, 137 (2000).
[9] D. Jung, Ph.D. thesis, Department of Mechanical and Aerospace Engineering, State University of New York at Buffalo, 2001.
[10] D. Jung, S. Gamard, W. K. George, and S. H. Woodward, "Downstream evolution of the most energetic POD modes in the mixing layer of a high Reynolds number axisymmetric jet," in *Turbulent Mixing and Combustion*, edited by A. Pollard and S. Candel (Kluwer, Dordrecht, 2002), pp. 23–32.
[11] L. S. Ukeiley, J. M. Seiner, and M. K. Ponton, "Azimuthal structure of an axisymmetric jet mixing layer," in ASME FEDSM99-7252, 1999.
[12] H. J. Hussein, S. P. Capp, and W. K. George, "Velocity measurements in a high-Reynolds-number, momentum-conserving, axisymmetric, turbulent jet," J. Fluid Mech. **258**, 31 (1994).
[13] N. R. Panchapakesan and J. L. Lumley, "Turbulence measurements in axisymmetric jets of air and helium, part 2 helium jets," J. Fluid Mech. **246**, 225 (1993).
[14] M. G. Mungal and D. K. Hollingsworth, "Organized motion in a very high Reynolds number jet," Phys. Fluids A **1**, 1615 (1989).
[15] P. E. Dimotakis, R. C. Miake-Lye, and D. A. Papantoniou, "Structure and dynamics of round turbulent jets," Phys. Fluids **26**, 3185 (1983).
[16] M. Yoda, L. Hesselink, and M. G. Mungal, "The evolution and nature of large-scale structures in the turbulent jet," Phys. Fluids A **4**, 803 (1992).
[17] M. Yoda, L. Hesselink, and M. G. Mungal, "Instantaneous three-dimensional concentration measurements in the self-similar region of a round high-Schmidt-number jet," J. Fluid Mech. **279**, 313 (1994).
[18] J. Tso and F. Hussain, "Organized motions in a fully developed turbulent axisymmetric jet," J. Fluid Mech. **203**, 425 (1989).
[19] G. K. Batchelor and E. A. Gill, "Analysis of the instability of axisymmetic jets," J. Fluid Mech. **14**, 529 (1962).
[20] A. Michalke, "On the inviscid instability of the hyperbolic-tangent velocity profile," J. Fluid Mech. **19**, 543 (1964).

[21]A. Michalke, ''On spatially growing disturbances in an inviscid shear layer,'' J. Fluid Mech. **23**, 521 (1965).
[22]A. Michalke, ''Survey on jet instability theory,'' Prog. Aerosp. Sci. **21**, 159 (1984).
[23]M. N. Glauser and W. K. George, ''Application of multipoint measurements for flow characterization,'' Exp. Therm. Fluid Sci. **5**, 617 (1992).
[24]J. H. Citriniti and W. K. George, ''The reduction of spatial aliasing by long hot-wire anemometer probes,'' Exp. Fluids **23**, 3, 217 (1997).
[25]W. K. George, ''Insight into the dynamics of coherent structures from a proper orthogonal decomposition,'' in *The Structure of Near Wall Turbulence, Proceedings of Symposium on Near Wall Turbulence*, Dubrovnik, Yugoslavia, edited by S. Kline (Hemisphere, New York, 1988), pp. 168–180.
[26]P. Holmes, J. L. Lumley, and G. Berkooz, *Turbulence, Coherent Structures, Dynamical Systems and Symmetry* (Cambridge University Press, Cambridge, 1996).
[27]W. K. George, ''Some thoughts on similarity, the POD, and finite boundaries,'' in *Trends in Mathematics, Proceedings of the Second Monte Verita Colloquium*, edited by A. Gyr and A. Tsinober (Birkhauser, Sweden, 1999).
[28]D. Ewing, Ph.D. thesis, Department of Mechanical and Aerospace Engineering, State University of New York at Buffalo, 1995.
[29]S. Gamard and W. K. George, ''Application of the POD to the similarity region of an axisymmetric turbulent jet,'' in Proceedings of the ASME Fluids Engineering Division Summer Meeting, Montreal, Quebec, Canada, July 2002.
[30]J. L. Lumley, ''On the interpretation of time spectra in high intensity shear flows,'' Phys. Fluids **8**, 1056 (1965).
[31]J. A. B. Wills, ''On convection velocities in turbulent shear flows,'' J. Fluid Mech. **20**, 417 (1964).
[32]K. B. M. Q. Zaman and A. K. M. F. Hussain, ''Taylor hypothesis and large-scale coherent structures,'' J. Fluid Mech. **112**, 379 (1981).
[33]P. Johansson, W. K. George, and S. H. Woodward, ''Proper orthogonal decomposition of an axisymmetric turbulent wake behind a disk,'' Phys. Fluids **14**, 2508 (2002).
[34]V. F. Kopiev, M. Yu Zaitsev, S. A. Chernyshev, and A. N. Kotova, ''The role of large-scale vortex in a turbulent jet noise,'' AIAA Pap. 99-1839 (1999).
[35]P. J. Morris, M. G. Giridharan, and G. M. Lilley, ''On the turbulent mixing of compressible free shear layers,'' Proc. R. Soc. London, Ser. A **431**, 219 (1990).
[36]Y. Y. Chan, ''Spatial waves in turbulent jets,'' Phys. Fluids **17**, 46 (1974).